frontiers | Frontiers in Earth Science

ORIGINAL RESEARCH
published: 25 April 2022
doi: 10.3389/feart.2022.884971

Structural Analysis and Evolution Model of the Longmaxi Formation in the Yanjin–Junlian Area of the Southern Sichuan Basin, China

Huaimin Wang[1], Cunhui Fan[1], Yi Fang[1], Shengxian Zhao[2], Xiangchao Shi[3], Jianfeng Liu[4], Hongfeng Yang[5], Jun Hu[6] and Chengbo Lian[1]*

[1]School of Geoscience and Technology, Southwest Petroleum University, Chengdu, China, [2]Shale Gas Research Institute, PetroChina Southwest Oil & Gas Field Company, Chengdu, China, [3]State Key Laboratory of Oil and Gas Reservoir Geology and Exploitation, Southwest Petroleum University, Chengdu, China, [4]Water Resources and Hydropower, Sichuan University, Chengdu, China, [5]Earth System Science Programme, The Chinese University of Hong Kong, Shatin, China, [6]Geomathematics Key Laboratory of Sichuan Province, Chengdu University of Technology, Chengdu, China

OPEN ACCESS

Edited by:
Shu Jiang,
The University of Utah, United States

Reviewed by:
Zhu Baiyu,
Yangtze University, China
Ruyue Wang,
Sinopec Petroleum Exploration and Production Research Institute, China
Hucheng Deng,
Chengdu University of Technology, China

***Correspondence:**
Cunhui Fan
fanchswpi@163.com

Specialty section:
This article was submitted to Economic Geology, a section of the journal Frontiers in Earth Science

Received: *27 February 2022*
Accepted: *24 March 2022*
Published: *25 April 2022*

Citation:
Wang H, Fan C, Fang Y, Zhao S, Shi X, Liu J, Yang H, Hu J and Lian C (2022) Structural Analysis and Evolution Model of the Longmaxi Formation in the Yanjin–Junlian Area of the Southern Sichuan Basin, China. Front. Earth Sci. 10:884971. doi: 10.3389/feart.2022.884971

The Longmaxi Formation in the southern Sichuan Basin is an important target for shale gas exploration and development. The characteristics and stages of structural development significantly impact shale gas preservation and enrichment. Taking the Longmaxi Formation in the Yanjin–Junlian area of the southern Sichuan Basin as an example and based on the results of surface and underground structural analysis, fluid inclusion tests, apatite fission track experiments, and burial-thermal evolution history analysis, a comprehensive study of the development characteristics and structural stages of the Longmaxi Formation was carried out, and an evolution model was developed. (1) The Longmaxi Formation of the Yanjin–Junlian area has been affected by multistage structural movements and exhibits structural compounding and superposition corresponding to different stages. The formation of surface tracks of the folds and faults has been affected by multidirectional extrusion stresses of the near SN, NE, and near EW. There are three stages of underground faults in the Longmaxi Formation, and the strikes are nearly EW, NE, and nearly SN. (2) Three distribution intervals for the homogenization temperature ranges of fracture fillings are 161–195°C, 121–143°C, and 74–105°C. The apatite thermal history simulation reveals that the Longmaxi Formation experienced three stages of tectonic movement after its formation. (3) There were clearly three stages in the structural development of the Longmaxi Formation in this area: the late Jurassic–Palaeocene (55 ± 5–38 ± 2 Ma), Eocene–early Miocene (38 ± 2–15.5 ± 3.5 Ma), and late Miocene-present (15.5 ± 3.5 Ma–present). Thus, a compound fracture system with superimposed structural deformations in different directions and at different stages formed in the study area. (4) A model for the stages and development of structural tracks in the Longmaxi Formation was established in conjunction with structural analysis and geomechanical theory. The results have guiding significance for the evaluation of shale gas preservation conditions and accumulation in the study area.

Keywords: structural analysis, structural track, evolution model, Longmaxi formation, shale gas, Yanjin-Junlian area

INTRODUCTION

In recent years, shale gas exploration and development has become an active area in global oil and gas exploration. North America has taken the lead in realizing efficient commercial exploitation of shale gas, which has changed the global oil and gas supply pattern and promoted the development of shale gas geological theory (Melchin and Holmden, 2006; Li et al., 2019a; Fan et al., 2020a; He et al., 2021; Ma et al., 2021; Zhang et al., 2022). China is among the countries that have implemented the exploration and development of shale gas resources outside North America, and the shale in the Southern Marine Silurian Longmaxi Formation is the main strata for shale gas exploration and development (Nie and Jin 2016; Shi et al., 2016; Nie et al., 2018, 2020; Zhu et al., 2022). Compared with marine shale in North America, marine shale in southern China has undergone structural activities at multiple stages over a long-term evolution history, resulting in complex preservation conditions for shale gas. A high total organic carbon (TOC) content, high brittleness, high formation pressure, and structural preservation conditions are known to be the dominant factors affecting the enrichment and high production of shale gas fields (Ambrose et al., 2010; Hou et al., 2020; He et al., 2021; Song et al., 2021; Li et al., 2022a; 2022b; Li 2022a; 2022b). Structural preservation conditions include indicators such as folds, faults, fractures, structural styles and deformation strengths. Structural preservation conditions control the enrichment degree of shale gas, which is one of the determining factors in shale gas exploration and development (Curtis, 2002; Jarvie et al., 2007; Qie et al., 2021; He et al., 2022a; 2022b). Among these conditions, the development of faults and fractures is an important index parameter for shale gas preservation (Hooker et al., 2018; Cheng et al., 2021). Faults control the development of fractures, which may become escape channels for shale gas. Second- and third-level faults have a destructive effect on oil and gas preservation conditions, while fourth-level faults can be used as channels for oil and gas migration. When the fracture strike and the current horizontal principal geostress intersect at a high angle, the high fault sealing performance inhibits the escape of shale gas (Wang et al., 2018, 2019; Xu et al., 2020; Shan et al., 2021; Wang and Wang 2021). In addition, the dominant orientation and development degree of the fractures formed in different structural evolution stages are different, and their effects on the enrichment and gas bearing properties in the later stage are also different. The structural stage matching the shale gas accumulation stage is of great significance for the enrichment of shale gas. Faults and fractures are important structural traces and the result of the comprehensive action of the palaeotectonic stress field (Yan et al., 2009; Li et al., 2012; Zhang et al., 2020a; 2020b). The analysis of structural traces is of great significance in terms of studying the action mode of regional tectonic stress fields, exploring the relationship between tectonic deformation and the stress state, and studying the mechanism of tectonic formation.

The Yanjin–Junlian area is located at the intersection of the southern Sichuan fold belt and the Loushan fault-fold structural belt, close to the edge of the basin. The Longmaxi formation shale is an important exploration layer, but shale gas exploration has not made an important breakthrough in recent years. Compared with the adjacent Changning block, its gas content and single-well production are poor, and the structural preservation conditions may be an important factor. Therefore, starting with macro geological analysis (similar outcrops, cores, and geophysical interpretation) and micro experimental tests (apatite fission track analysis, inclusion temperature analysis, and burial-thermal evolution history) (Li et al., 2020), this paper analyses the formation stage and evolution model of the structure in the study area to provide guidance for shale gas exploration in this and similar basin margin areas.

GEOLOGICAL BACKGROUND

The Yanjin–Junlian area is located at the southern edge of the Sichuan Basin, at the intersection of the southern Sichuan fold belt and the Loushan fault-fold structural belt (**Figure 1A**). The Yanjin–Junlian area is adjacent to the Dawan Anticline and the Tianningsi Structure in the east of the basin, the Xunsifang and Junlian Nose Structures in the area west of the basin, the Datianba Anticline in the area south of the basin, and the Luochang, Fujiang Syncline, and Tiancun Anticline in the area north of the basin. The eastern and western parts of the study area have been regionally affected by the long-distance transmission of extrusion stress originating from the Jiangnan Xuefeng Uplift and Longmen Mountains, respectively, whereas the northern and southern parts have been affected by compression from the Huayingshan–Qingshanling Fault Zone and the Daloushan Structural Belt, respectively (Fan et al., 2018, 2020b; Xie et al., 2019; Wang et al., 2020). Different complex structural tracks have been constrained and superimposed on each other.

During the sedimentary period of the Longmaxi Formation in the early Silurian, the entire southern Sichuan area was constrained by the central Sichuan Palaeohigh and the central Guizhou Palaeohigh, creating an overall continental shelf sedimentary environment. The Longmaxi Formation is generally divided into upper and lower sections (Yang et al., 2017; Jin et al., 2018). The lithology of the upper section is primarily light grey silty mudstone or argillaceous silt, with a thickness of approximately 90–210 m. The lower section is dominated by dark grey–black mud shale with a thickness of approximately 65–240 m, and a set of organic-rich shales with TOC>2% (average > 3.5%) and thicknesses of 20–50 m have developed at the bottom, which is currently the main gas production layer for shale gas exploitation (**Figure 1B**). These shales have been affected by multistage structural activities and the superposition of two structural domains, i.e., the Tethys and Marginal-Pacific Oceans, and therefore have a complex structural track and developed faults and fractures, which significantly impact the preservation and enrichment of shale gas.

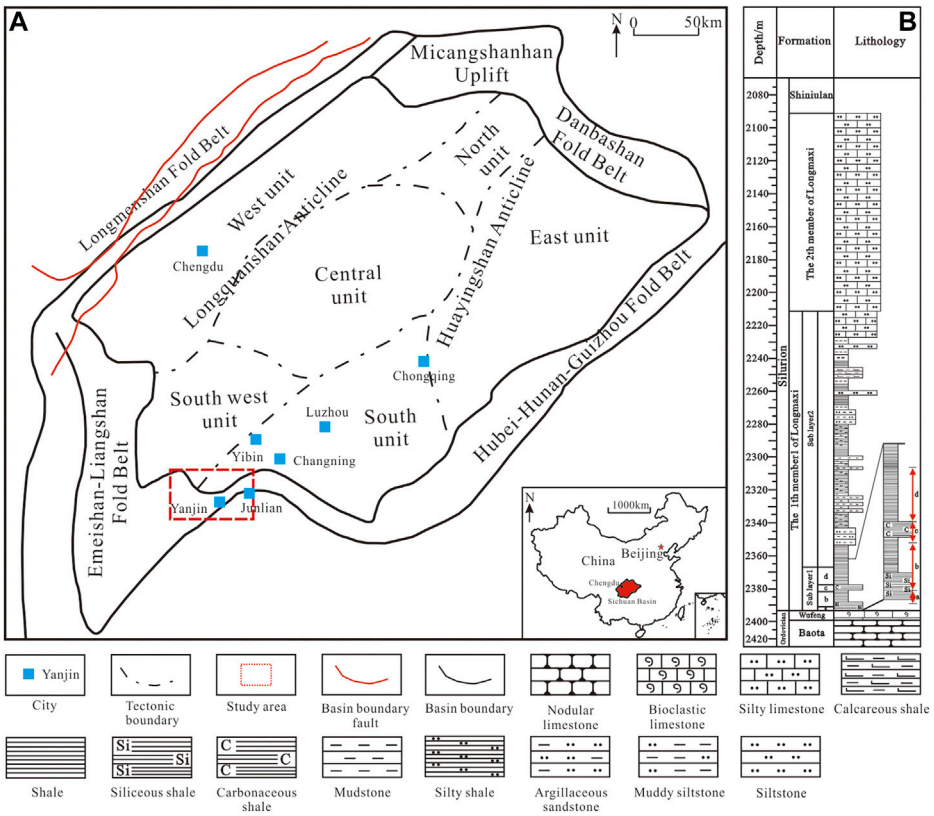

FIGURE 1 | Geological overview of the Yanjin–Junlian area (Zhang et al., 2021). **(A)**. Structural location; **(B)**. stratigraphic histogram.

SAMPLES AND METHODS

Samples

Two main methods were used in this study: macrogeological analysis and microexperimental testing. In the macrogeological analysis, field outcrop surveys, drilling core observations, formation microresistivity imager (FMI) image logging and seismic structure analysis were combined with actual production data analysis. A fracture investigation and statistical analysis were conducted at eight observation points in the outcrop area of the Yanjin Anticline, and a total of 385 sets of fracture data and 169 photos were collected. Core observation and sampling were conducted in the Longmaxi Formation at a depth of approximately 178.64 m in wells N219, N228, etc., and 35 fracture filling samples and 12 full-diameter samples were obtained. In addition, 1020-km^2 three-dimensional (3D) seismic data volumes were collected from the Shuanglong–Luochang area for structural interpretation.

Macrogeological Analysis Methods

Considering the regional structural background, a fracture investigation was conducted on well-exposed strata of the Yanjin Anticline Longmaxi Formation outcrop, and the fractures were staged and supported. Drilling core observations were primarily used to determine the fracture type, development degree, filling characteristics, fracture intersection relationship, etc. FMI logging was used to recognize and interpret fracture occurrence (Fan et al., 2020a, 2020b; Li et al., 2020; Li, 2021). The LANDMAK 2003.12.13 interpretation system and 10 × 10 survey network density controls were employed to process and interpret the 3D seismic data from the Shuanglong–Luochang area, and these data were used to determine the fracture distributions, intersection relationships, and evolution processes at different stages.

Microexperimental Testing Methods

Inclusion Testing of Fracture Filling

Homogenization temperature tests were performed on the primary mineral inclusions that formed during the same stage as the fracture filling. The homogenization temperature distribution intervals of the inclusions showed that the fractures and fracture formation stages played a critical role during the paleostructural period. Fifteen fracture filling samples from four wells in the study area were formed into rock slices. The slices were placed on a THMSG600 geological cold-and-hot platform at room temperature and heated at a rate of 2°C/min until the gas–liquid inclusions were homogenized. The homogenization temperatures were then recorded. Statistical data were collected on the homogenization temperatures of all fluid inclusions. The characteristics of the inclusions and

homogenization temperature intervals were used to identify the fluid-filling stages (Li et al., 2019b).

Analysis of the Thermal Evolution Degrees of Organic Matter

An Axioscope. A1 polarized light microscope and an MSP.400 microspectrophotometer were used for testing. The experimental samples were placed on the microscope stage, and the asphalt reflectance (R_o) was measured under unpolarized light. The asphalt reflectance of the test sample was measured and converted to the equivalent vitrinite reflectance (R_{ob}) using a relationship established by Feng et al. ($R_o = 0.6569 \times R_{ob} + 0.3364$, natural series).

Low-Temperature Thermochronology and Thermal History Simulation of Apatite

Radiation damage was experimentally assessed based on 238U spontaneous fission effects. The low-temperature thermal evolution history of rocks was simulated using mathematical geological models that can effectively reveal the history of basin structural uplifts and denudation (Reiners, et al., 2004; Deng et al., 2013). Due to the lack of apatite heavy minerals in the fine-grained rocks of the Longmaxi Formation and according to the principle that continuous strata have similar thermal evolution histories, fresh Jurassic coarse sandstone samples from the surface of the Junlian area were selected for apatite fission track testing and thermal history simulation.

RESULTS

Macrogeological Method Stage Study

Analysis of Surface Fold Structure

Structural superposition and transformation are the most direct and effective evidence for use in structural analysis and to determine structural development sequences (Schwartzkopff et al., 2017; Li et al., 2019b). The sequences of structural activities during different periods can be determined from the spatial intersections and compounding relationships of structural tracks formed by these structural activities.

The study area is located at the intersection of the southern Sichuan fold belt and the Loushan fault-fold structural belt. The area has been transformed by structural actions at different stages and in different directions and thus exhibits the characteristics of structural compounding and superposition at different stages. Using fold development as a barometer, the Yanjin Anticline and Luochang Syncline main structural bodies are characterized as ENE-trending, the northern Changning Anticline and other structural bodies are characterized as WNW-trending, and the northwestern Fujiang Syncline, Tiancun Anticline, and other main structural bodies are characterized as NW-trending. However, the structural tracks of adjacent areas are quite dissimilar. The central main body of the Yanjin Anticline is ENE-trending and turns eastward towards the nearly SN-trending Junlian–Shuanghe Anticline, thereby counteracting the arc-shaped axis that turns from EW to NW towards the Zhonghechang Anticline to the west, and this anticline exhibits prominent structural superposition characteristics (**Figure 2**). The SN-trending structures are superimposed on early ENE-trending structures, and the main body of the Luochang Syncline is ENE-trending, which transforms northwest to the NE-trending Fujiang Syncline. The fold structure track shows that the surface structure has clearly been affected by extrusion stress in three directions, for which the sequence is near SN, NE, and near EW.

Analysis of Surface Outcrop Fractures

Field fracture observations were primarily conducted on the Longmaxi Formation stratum exposed by the Mitanzi Anticline, including eight observations, i.e., Huangjiaping, Longdong Village, Banbiandu, Gaoshikan, Lijiawan, Xinhua Village, Lantian, and Diaolouzi. A total of 446 sets of fracture orientation observation data were obtained.

There are plane shear fractures, sectional shear fractures, and a few tension fractures in the Longmaxi Formation shale in the field outcrops. The shear fractures are widely developed, generally on the two wings of the anticline and the turning end of each observation point. The plane shear fracture intersects with the rock layer vertically or at a high angle. The fracture surface is straight, and the occurrence is relatively stable. The fracture often occurs as a planar X-shaped conjugate (**Figures 3A–D**). The sectional shear fracture intersects with the rock layer at a low angle and has a poor development degree compared with the plane shear fractures (**Figures 3E,F**) (Yin and Wu 2020; Li, 2021; Yu et al., 2021). The tension fractures are geometrically irregular, with large variations in width and a short extension. When the formation was deposited, the stratum dip angle changed due to transformations under subsequent tectonic stress, and the fracture occurrence from the early stage changed accordingly. Therefore, the fracture occurrence measured in the field corresponds to that after structural deformation of the stratum during the later stage. The development orientation of the conjugate shear fractures before and after layer correction was compared, and fracture staging and supporting analysis were performed to identify the fracture stages of the Longmaxi Formation. StrGraphPrj software was used for layer correction, and DIPS geological geometry analysis software was used to perform a statistical analysis based on the strike rose diagram, stereographic projection, and other layer correction methods to determine the dominant orientation of cracks (Laubach et al., 2009; Ameen 2016).

Based on structural geology principles, the intersection line of a conjugate shear fracture is parallel to the middle principal stress axis, and the maximum principal stress axis and the minimum principal stress axis are parallel to the angular bisectors of the included acute angle and the included obtuse angle, respectively (Li et al., 2019b, 2022a; Gao 2019; Kang, 2021). The direction of the principal stress can thereby be determined. There are six groups of planar X-shaped conjugate shear fractures and three groups of sectional shear fractures in the Longmaxi Formation shale (**Figure 4**), where the SSW-trending (195° ± 10°) and SE-trending (145° ± 5°) fractures constitute early planar X-type conjugate shear fractures that formed by strong horizontal extrusion by the Daloushan Fold Belt from SSW to NNE (175° ± 5°). In the later stage of structural action, near-EW-

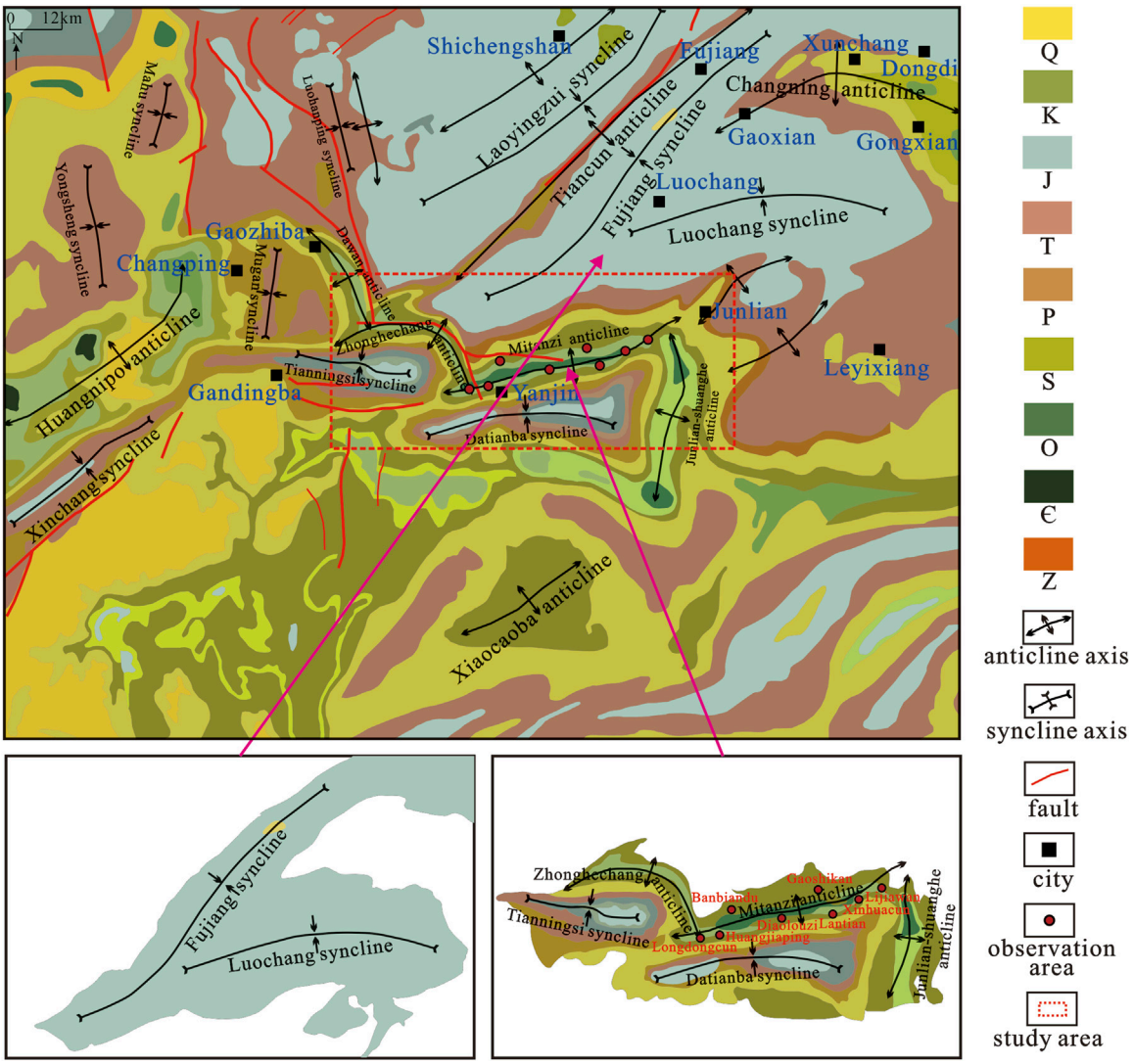

FIGURE 2 | Tracks of surface fold structures in the Shuanglong–Luochang area.

trending (265° ± 5°) sectional shear fractures formed, and the WNW-trending (285° ± 5°) and NE-trending (35° ± 5°) fractures constituted second-stage planar X-shaped conjugate shear fractures. These shear fractures were formed slightly later than the SSW- and SE-trending fractures by NW-trending (315° ± 10°) extrusion caused by the joint actions of the central Sichuan Uplift and Jiangnan Xuefeng Uplift, and NE-trending (35° ± 5°) sectional shear fractures also formed. The SW-trending (235° ± 5°) and NW-trending (305° ± 5°) fractures constitute the last-stage planar X-shaped conjugate shear fractures and have the longest formation time, primarily resulting from the extrusion stress in the near-EW direction (265° ± 5°). A few near-SN-trending (355° ± 5°) sectional shear fractures developed.

Core Fracture Staging and Support

The clear relationship among core fracture development, core fracture shape, filling material, and intersection development of core fractures in the Longmaxi Formation provides data for directly determining the structural stages. The structural fractures in the Longmaxi Formation are dominated by high-angle and vertical-shear fractures. The shear fractures are characterized by stable occurrences, smooth fracture surfaces, and clear intersection relationships. Intersection relationships at three stages can be clearly seen (**Figure 5**). The dominant FMI imaging logging fracture trends are near EW (85° ± 10°), NNE (35° ± 5°) and WNW (285° ± 5°), followed by NW (335° ± 5°), NW (290° ± 5°), and ENE (75° ± 5°) (**Figure 6**). The FMI log for each well is limited by the structural position at the drilling location, the size of the wellbore, and the imaging range and therefore only reflects the fracture development around the wellbore and not the overall development of underground fractures. The fractures in each well have different dominant orientations, which are included in the dominant orientations of the outcrop fracture ranges, and there is a correspondence

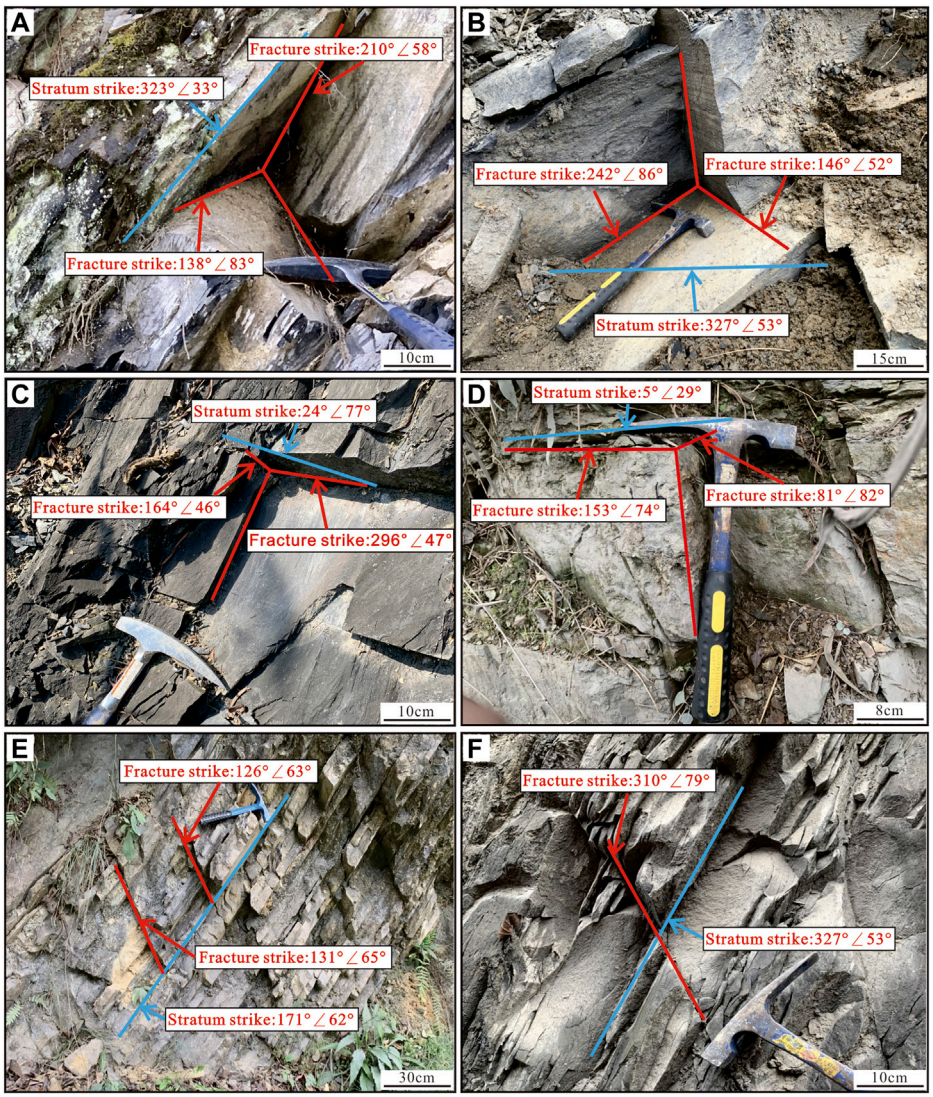

FIGURE 3 | Types and characteristics of fractures of Longmaxi Formation in outcrops. **(A)**. Plane shear fracture, Gaoshikan area; **(B)**. plane shear fracture, Banbiandu area; **(C)**. plane shear fracture, Huangjiaping area; **(D)**. plane shear fracture, Lantian area; **(E)**. profile shear fracture, Diaolouzi area; **(F)**. profile shear fracture, Banbiandu area.

between the downhole orientations and surface fracture orientations.

Fault Structure Analysis of the Longmaxi Formation

The fracture system in the study area was formed under the constraints imposed by the tectonic stress field in southeastern Sichuan and is consistent with the evolution sequence by which it originated. Therefore, a structural evolution model can be developed based on the underground fault characteristics of the Longmaxi Formation.

The geophysical interpretation shows that the faults of the Longmaxi Formation in the study area are primarily NE, near SN and NW, with a few near-EW faults. Most faults have dips between 40 and 60° and appear as reverse faults on the seismic sections (**Figure 7**). Consistent with the study of core and outcrop fractures, the intersection and restriction relationship of faults on the plane can also be used to analyse the structural stage (Feng et al., 2018; Yu et al., 2022). In addition, structural traces of the folds are also the basis for macro analysis of structural stages (**Figure 8**). There are only two EW-trending faults, both of which occur in the southern part of the study area, and the fault direction is consistent with the extension direction of the Yanjin Anticline. This fault formed the earliest in the study area and has a formation time consistent with that of the near EW-trending Yanjin Anticline. The NE-trending faults are the most developed in the study area: these faults obliquely intersect the main fold structural tracks, and their tracks are consistent with the NE-trending superimposed structures, such

Location	Stratum strike	Dominant strike data		Strike rose diagram of the fractures (after strike recover)	The overall strike rose diagram of the fractures in the study area (after strike recover)
		Plane shear fracture	Profile shear fracture		
Huangjiaping	190°∠61°	54°∠79° 147°∠83°	124°∠73°	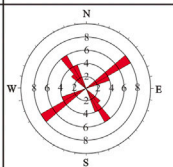	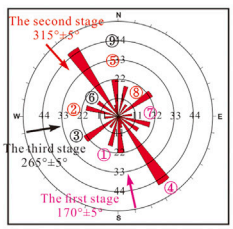 Dominant strike of plane shear fracture. SSW(195°±10°) NWW(285°±5°) SW(235°±5°) SE(145°±5°) Near NS(355±5°) NW(305°±5°) Dominant strike of profile shear fracture. Near EW(265°±5°) NE(35°±5°) Near SN(355°±5°)
Longdongcun	261°∠64°	357°∠84° 315°∠81°	236°∠72°	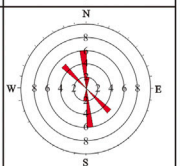	
Banbiandu	327°∠53°	27°∠80° 54°∠82° 325°∠74°	127°∠83°	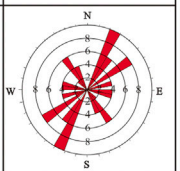	
Gaoshikan	323°∠33°	57°∠76° 113°∠69°	119°∠69°	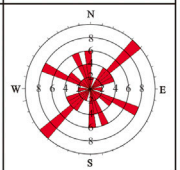	
Lijiawan	24°∠77°	161°∠77° 79°∠82° 56°∠81°	246°∠80°	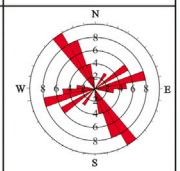	
Xinhuacun	337°∠74°	322°∠83° 87°∠76° 104°∠80°	132°∠77°	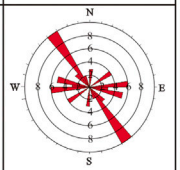	
Lantian	5°∠29°	353°∠77° 78°∠81°	118°∠81°	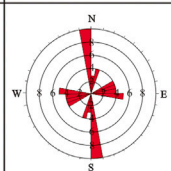	
Diaolouzi	171°∠62°	18°∠81° 53°∠77° 105°∠80° 147°∠82°	126°∠76°	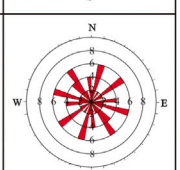	

FIGURE 4 | Staging and supporting outcrop fractures in the Longmaxi Formation in the Yanjin–Junlian area.

as the Fujiang Syncline and Zhonghechang Anticline in the west. These tracks would have formed under structural movements during the second stage, and the near-SN-trending faults only developed in the western part of the study area near the basin margin and turned eastward to become NW-trending. The tracks of the faults at this stage are consistent with the near-SN-trending Junlian–Shuanghe Anticline and result from previous structural movement. Based on the regional

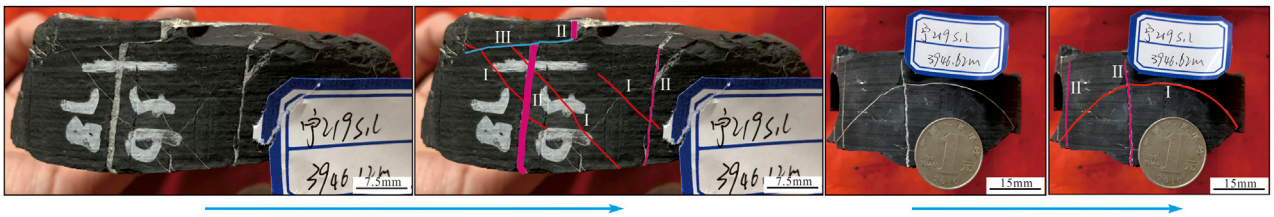

FIGURE 5 | Developmental characteristics and intersection relationship of core fractures.

structural background and extrusion stress mechanisms, the structural evolution of the Yanjin–Junlian area has primarily been affected by three stages of structural movement: the near-EW structure formed first, followed by the NE-trending structure, and then the near-SN-trending structure (which turned eastward towards the NW-trending structure), which is consistent with the analytical results for the surface structural tracks.

Experimental Testing Methods

Inclusion Testing for Fracture Filling

The results from inclusion homogenization temperature tests on different core fracture fillings, the core fracture cutting relationship, and the FMI imaging interpretation results were used to identify three categories of fractures in the Longmaxi Formation downhole; that is, these fractures were affected by three stages of structural movement (**Figure 9**) (Burruss et al., 1983; Mourgues et al., 2012; Han et al., 2018). The inclusions of the first-stage fracture fillings are two-phase (gas–liquid), with a gas–liquid ratio of 5–8%, corresponding to the first-stage structural uplift at the maximum burial depth of the study area. The homogenization temperature is in the 161–195°C range, which is the highest among the three stages. The second-stage fractures are filled with coarse-grained calcite, dominated by semifilling or nonfilling, and the inclusions are primarily distributed in groups. The homogenization temperature is primarily in the 121–143°C range. The third-stage fractures have a low filling degree, and the homogenization temperature is low (primarily in the 74–105°C range), indicating that the uplift reaches the maximum extent at this time, the burial depth is shallow, and the structure is basically finalized.

Burial-Thermal Evolution History Analysis

Burial-thermal evolution history analysis was used to accurately determine the uplift and subsidence history of the Longmaxi Formation since the sedimentary period of the Changyanjin–Junlian area, which reflects the formation time of the fractures in the Longmaxi Formation. The burial-thermal evolution history was determined using the drilling geological data, regional heat flow value, rock thermal conductivity, and geochemical experimental test data for Well N221 (Yin et al., 2018; Fan et al., 2020b; Li et al., 2020). Five major structural uplifts have occurred in the study area since the Caledonian period. The first stage is the early Caledonian–Hercynian movement (415–270 Ma), which is the overall uplift stage, and the burial depth is generally within 1900 m. The second stage is in the early stage of the Hercynian–Yanshan movement (260–50 Ma), which involved continuously descending sediment. The burial depth is between 2000 and 6,000 m. The third stage is in the late Yanshan movement (50–37 Ma), during which strong uplift and denudation occurred, and the burial depth is between 4,800 and 5,800 m. The fourth stage is in the early-middle period of the Himalayan movement (37–20 Ma), during which rapid uplift and denudation occurred. The burial depth is 3,500–4,500 m. The fifth stage is in the late Himalayan movement (19 Ma–0), a stage of continuous extrusion and uplift, with a burial depth of 2,200–3,700 m (**Figure 10**).

The Ordovician (O)–Jurassic (J) strata in southern Sichuan are in conformity or parallel unconformity contact. Before the middle-late Yanshanian stage, only a relatively simple vertical up-and-down movement occurred in the study area that weakly influenced the structural track over the entire area. Therefore, the formation periods for the Longmaxi Formation in the Yanjin–Junlian area are the late Yanshan movement, the early-middle Himalayan movement, and the late Himalayan movement to the present. The first two structural movements are characterized by short durations and large uplifts. Thus, these strong structural movements were the most critical for forming structural tracks in the study area.

Low-Temperature Thermochronology and Thermal History Simulation of Apatite

Apatite fission track testing and thermal history simulations effectively revealed the history of structural uplift and denudation in the basin. The experimental test results presented in **Figure 10** show that the fission track length distribution of the experimental sample apatite is concentrated, the cooling age is 67.1 ± 5 Ma, the fission track length is 10.8 ± 4 μm, and the peak track length is 9–11 μm (**Figure 11**). The thermal history simulation of the apatite particles revealed that the strata samples in this area primarily underwent four thermal evolution stages. The first stage of uplift and denudation occurred during the Permian to Middle Jurassic (250–65 Ma), and rapid burial occurred after the Middle Jurassic sedimentary period. This simulation shows that the early fission tracks generated during the denudation process were not completely reset during the later burial process, and some thermal evolution information of the source region was preserved.

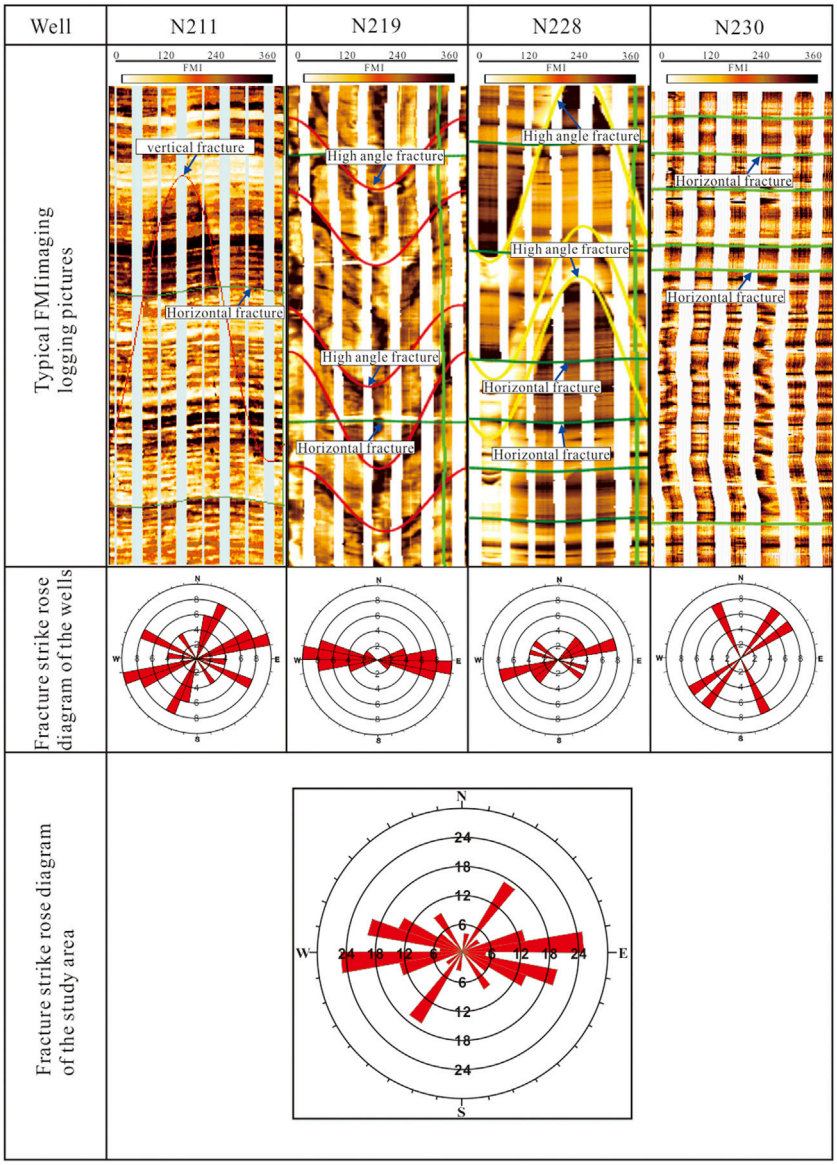

FIGURE 6 | Fracture characteristics and strike rose diagram from image logging.

The evolution stages after the late Yanshan period include the late Jurassic (60–40 Ma), Eocene–early Miocene (40–10 Ma), and the late Miocene–present (10 Ma–present). Although the fission track was not completely reset from the early Permian to the middle Jurassic (250–65 Ma), these results prove that the Longmaxi Formation primarily underwent three major structural movements after formation.

DISCUSSION

In this study, fracture staging was performed by combining geological methods, such as surface-outcrop fracture investigation, structural track analysis, downhole-core fracture description, and seismic and logging data analysis, with fracture-filling inclusion-homogenization-temperature testing, burial-thermal evolution history, apatite experimental fission tracks, and other experimental analysis methods (Ibrahim et al., 2017; Jiang et al., 2017; Feng et al., 2018; Smeraglia et al., 2021; Wang et al., 2022). The results confirmed that three primary stages of structural movement occurred after the sedimentary period of the Longmaxi Formation in the Yanjin–Junlian area, corresponding to three stages of structural evolution. The theory of structural geology and fracture mechanics was used to develop a structural evolution model for the Longmaxi Formation (**Figure 12**).

Before the early Yanshan structural movement (before 55 ± 5 Ma), the structural environment of the

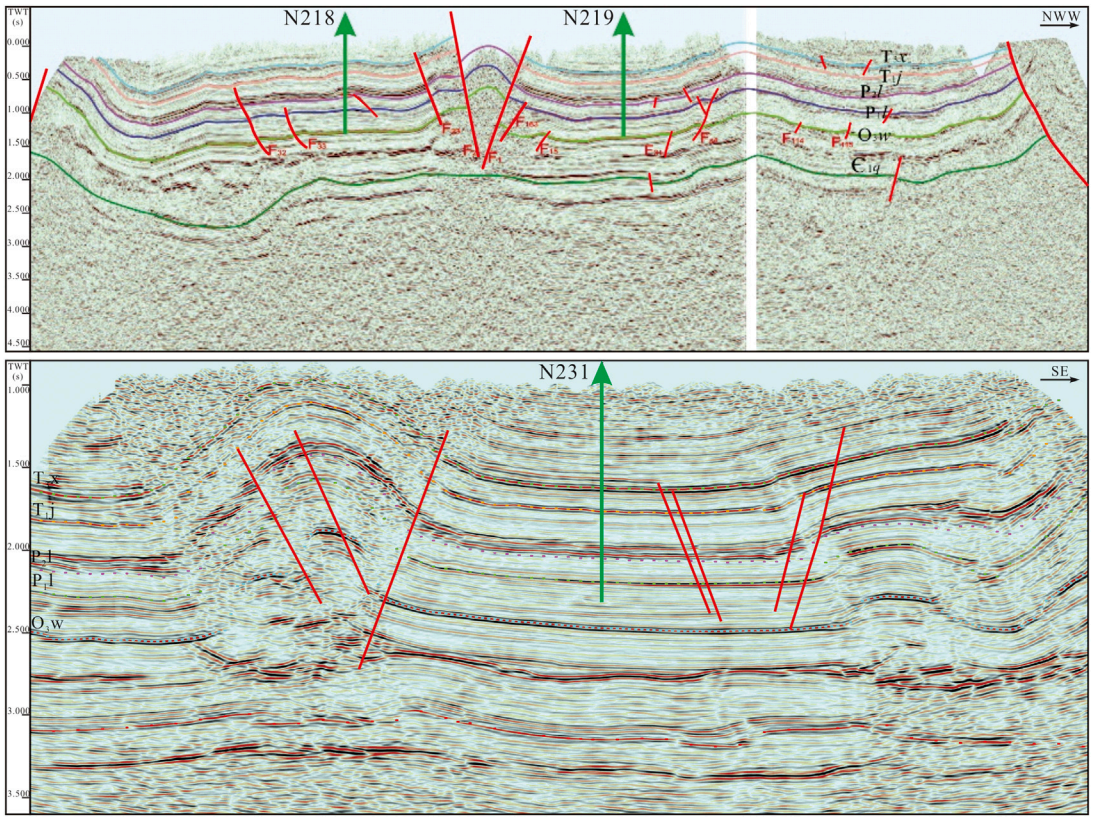

FIGURE 7 | Characteristics of the faults in seismic profiles.

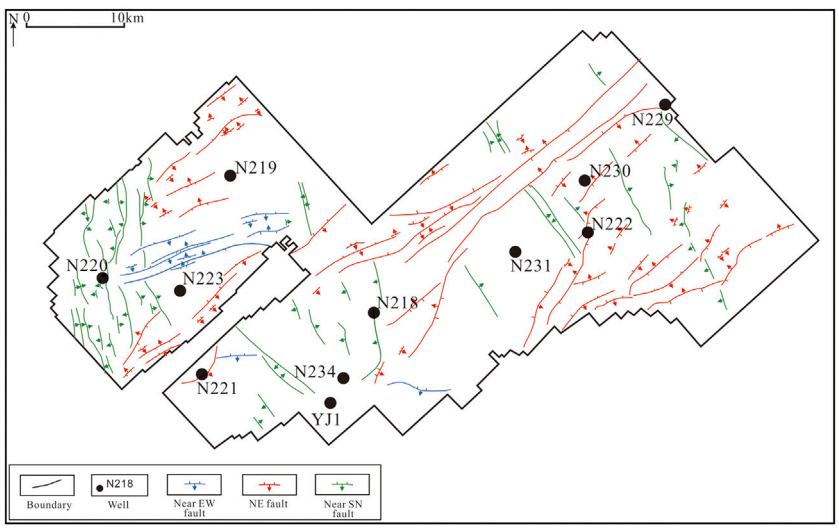

FIGURE 8 | Structural outline of the Longmaxi Formation in the Yanjin–Junlian area (seismic interpretation results).

Yanjin–Junlian area was relatively stable and primarily dominated by up-and-down movements. Strata from the Sinian to the Middle Jurassic were deposited from bottom to top. The structural movement at this stage had little effect on the development and structural track of the Yanjin–Junlian area.

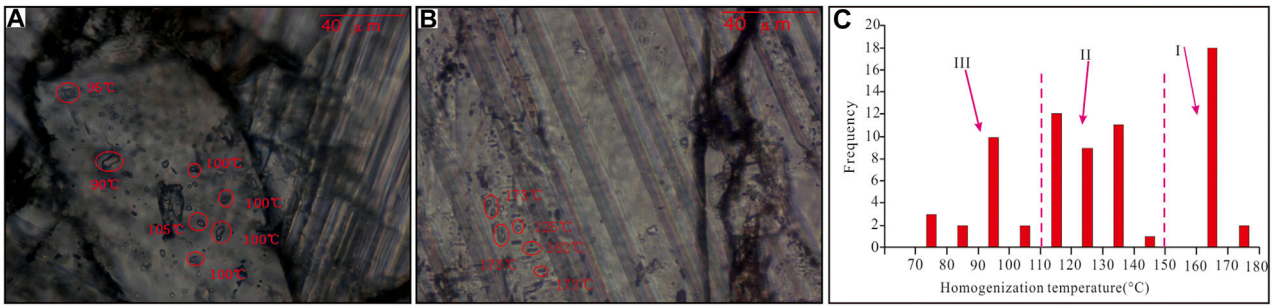

FIGURE 9 | Fluid inclusion characteristics of fracture fillings. **(A–B)** is fluid inclusion characteristics; **(C)**. The distribution range of homogenization temperature.

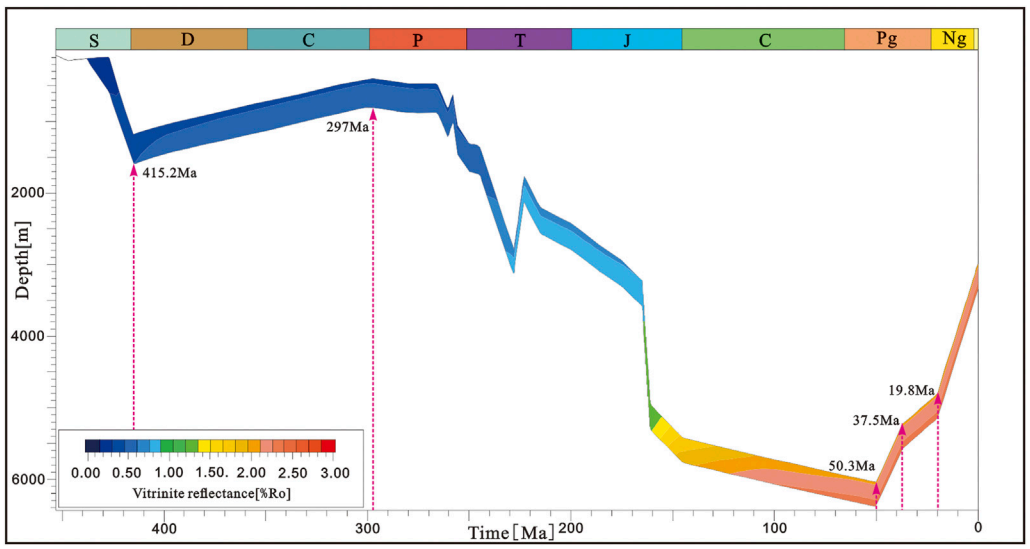

FIGURE 10 | Burial-thermal evolution history of Well N221.

Late Jurassic–Palaeocene (55 ± 5–38 ± 2 Ma): Extrusion of the near-SN-trending Daloushan Structural Belt (170° ± 5°) caused a group of NNW- and NE-trending planar shear fractures to develop in the study area before significant deformation of the Longmaxi Formation occurred. These fractures intersect at a high angle or are perpendicular to the layer and appear as X-shaped conjugate shear fractures on the plane. Continuous extrusion of tectonic stress at this stage resulted in the formation of near-EW-trending folds, such as the Yanjin Anticline and Luochang Syncline. Near-EW-trending sectional shear fractures were generated along with the strata fold deformations. The fractures further expanded and penetrated through the layer, forming a few near-EW-trending fractures. These fractures formed earliest and have a high filling degree. The filling material was primarily calcite, and the homogenization temperatures of the filling inclusions were 161–195°C.

Eocene–early Miocene (38 ± 2–15.5 ± 3.5 Ma): The Indian and Eurasian Plates gradually collided and closed, causing the uplift of the Qinghai-Tibet Plateau, triggering NW- (305° ± 5°) trending extrusion in this area and forming the Fujiang Syncline, further generating NE-trending folds, such as the Fujiang Syncline and Tiancun Anticline, superimposed on the Luochang Syncline while simultaneously forming NW- and near-EW-trending plane conjugate shear fractures and NE-trending sectional shear fractures. The NE-trending sectional shear fractures further extended and penetrated the layer, forming the NE-trending reverse fractures that developed in the study area. The homogenization temperatures of the fracture-filling inclusions produced at this stage of structural movement were 121–143°C.

Late Miocene–present (15.5 ± 3.5 Ma–present): The collision between the Indian and Eurasian Plates and the subduction of the Pacific Plate produced a structural force that gradually expanded into the Sichuan Basin, whereby the study area was subjected to dual stresses from the south and north (under the joint action of the Xuefeng Uplift, Central Sichuan Uplift, and Central Guizhou Uplift). The western edge was subjected to near-EW-trending (265° ± 5°) structural extrusion, resulting in the formation of the

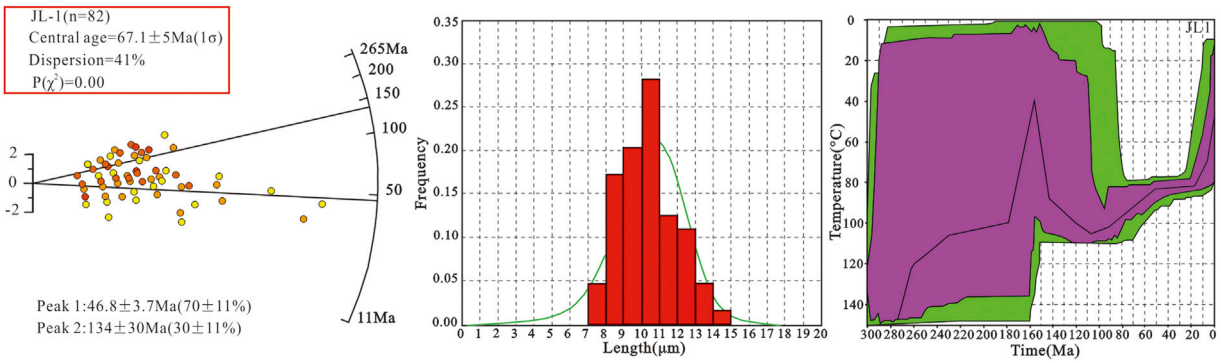

FIGURE 11 | Apatite fission track and thermal history simulation.

Stage		Orientation of stress field		Fracture orientation characteristic: Fracture dominant orientation	Fracture orientation characteristic: Orientation	Subsurface fault	Features of surface folds and faults
Indosinian stage and before	Ascending and descending motion						
Early Himalayan stage	①	Near NW (170°±5°)	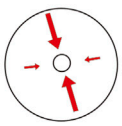		NNW and NE plane shear fractures and near EW profile shear fractures	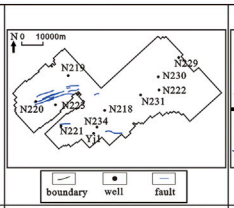	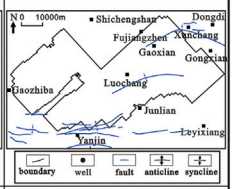
Early Himalayan - Middle Himalayan	②	NW (305°±5°)	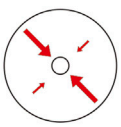	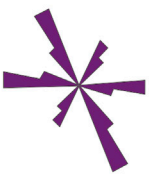	NW, near EW plane shear fractures, and NE profile shear fractures	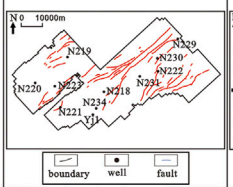	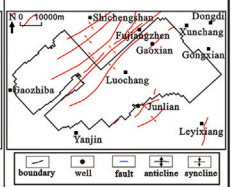
Middle Himalaya - Present	③	Near EW (265°±5°)	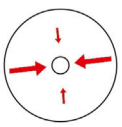		Near NWW NE plane shear fractures, and near SN profile shear fractures	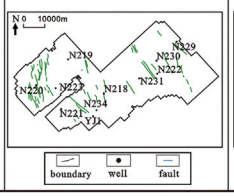	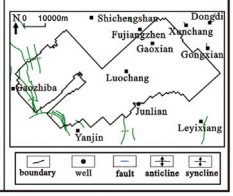

FIGURE 12 | Model for the structural development stages and evolution of the Wufeng-Longmaxi Formation in the Yanjin–Junlian area.

Junlian–Shuanghe Anticline superimposed on the Yanjin Anticline and Zhonghechang Anticline. During the tectonic stress transfer process influenced by the Xianshuihe left-lateral strike-slip fault zone, the tectonic stress was deflected from N to S in a counterclockwise direction, forming WNW- and NE-trending plane conjugate shear fractures in the north and near-SN-trending (NNW-trending) sectional shear fractures. During the fracture expansion processes at this stage, deflection of the stress field caused the formation of a near-SN-trending reverse fault in the north and the gradual formation of a WNW-trending reverse fault in the south. The fractures produced by the structural movement at this stage had a low degree of filling, and the homogenization temperatures of the filling inclusions were 74–105°C. The action of a later tectonic stress field resulted in the transformation and superimposition of the early structural track, and the system dominated by present NE- and near-SN-trending with a few near-EW-trending folds and fractures finally formed.

CONCLUSION

The Yanjin–Junlian Area in the southern Sichuan Basin was considered as a case study. A structural analysis was conducted using geological methods and experimental testing methods. The structural development characteristics, formation time, and sequence were determined, and then a structural evolution model of the Longmaxi Formation in the Yanjin–Junlian area was established.

(1) The Longmaxi Formation in the Yanjin–Junlian area of the southern Sichuan Basin is characterized by structural compounding and superposition from multistage structural movements. Based on the results of surface folding and fracture development, these movements were affected by SN, NE, and near EW extrusion stresses. The underground core fracture analysis and fault structure analysis results show that these movements have primarily developed in three directions, i.e., near EW, NE, and near SN, corresponding to the action of the main structural movements at three stages. The corresponding fractures also developed corresponding to the three stages.
(2) Fracture filling fluid inclusion tests, the burial-thermal evolution history, and apatite fission track tests confirmed that the formation of the structural track could be categorized into three main stages, i.e., the late Jurassic–Palaeocene (55 ± 5–38 ± 2 Ma), Eocene–Early Miocene (38 ± 2–15.5 ± 3.5 Ma), and late Miocene–present (15.5 ± 3.5 Ma–present). The homogenization temperatures of the fillings are 161–195°C, 121–143°C and 74–105°C. Finally, the tectonic evolution model of the Longmaxi Formation is established.

DATA AVAILABILITY STATEMENT

The original contributions presented in the study are included in the article/Supplementary Material, further inquiries can be directed to the corresponding author.

AUTHOR CONTRIBUTIONS

HW and CF contributed in writing, reviewing, and editing, data curation, writing-original draft preparation; YF, SZ, XS, JL, HY, JH, and CL contributed in formal analysis, validation, and reviewing.

FUNDING

This study was financially supported by the National Natural Science Foundation of China (Grant No. U20A20266).

ACKNOWLEDGMENTS

We thank all editors and reviewers for their helpful comments and suggestions.

REFERENCES

Ambrose, R. J., Hartman, R. C., Diaz-Campos, M., Akkutlu, I. Y., and Sondergeld, C. H. (2012). Shale Gas-In-Place Calculations Part I: New Pore-Scale Considerations. *Soc. Petrol. Eng.* 17 (1), 219–229. doi:10.2118/131772-PA

Ameen, M. S. (2016). Fracture Modes in the Silurian Qusaiba Shale Play, Northern Saudi arabia and Their Geomechanical Implications. *Mar. Pet. Geology.* 78, 312–355. doi:10.1016/j.marpetgeo.2016.07.013

Burruss, R. C., Cercone, K. R., and Harris, P. M. (1983). Fluid Inclusion Petrography and Tectonic-Burial History of the Al Ali No. 2 Well: Evidence for the Timing of Diagenesis and Oil Migration, Northern Oman Foredeep. *Geol* 11, 567–570. doi:10.1130/0091-7613(1983)11<567:fipath>2.0.co;2

Cheng, G., Jiang, B., Li, M., Li, F., and Zhu, M. (2021). Structural Evolution of Southern Sichuan Basin (South China) and its Control Effects on Tectonic Fracture Distribution in Longmaxi Shale. *J. Struct. Geology.* 153, 104465. doi:10.1016/j.jsg.2021.104465

Curtis, J. B. (2002). Fractured Shale-Gas Systems. *AAPG Bull.* 86 (11), 1921–1938. doi:10.1306/61eeddbe-173e-11d7-8645000102c1865d

Deng, B., Liu, S.-g., Li, Z.-w., Jansa, L. F., Liu, S., Wang, G.-z., et al. (2013). Differential Exhumation at Eastern Margin of the Tibetan Plateau, from Apatite Fission-Track Thermochronology. *Tectonophysics* 591, 98–115. doi:10.1016/j.tecto.2012.11.012

Fan, C. H., He, S., Zhang, Y., Qin, Q. R., and Zhong, C. (2018). Development Phases and Mechanisms of Tectonic Fractures in the Longmaxi Formation Shale of the Dingshan Area in Southeast Sichuan Basin, China. *Acta Geol. Sin.* 92 (6), 2351–2366. doi:10.1111/1755-6724.13732

Fan, C., Li, H., Qin, Q., He, S., and Zhong, C. (2020b). Geological Conditions and Exploration Potential of Shale Gas Reservoir in Wufeng and Longmaxi Formation of southeastern Sichuan Basin, China. *J. Pet. Sci. Eng.* 191, 107138. doi:10.1016/j.petrol.2020.107138

Fan, C., Li, H., Zhao, S., Qin, Q., Fan, Y., Wu, J., et al. (2020a). Formation Stages and Evolution Patterns of Structural Fractures in marine Shale: Case Study of the Lower Silurian Longmaxi Formation in the Changning Area of the Southern Sichuan Basin, China. *Energy Fuels* 34, 9524–9539. doi:10.1021/acs.energyfuels.0c01748

Feng, J., Chang, L., Zhao, L., and Li, X. (2018). Discrete Fracture Modeling of Deep Tight sandstone Reservoir Based on Convergent Multi-Information-A Case Study of KX Gas Field in Tarim Basin. *Arab. J. Geosci.* 11 (24), 804. doi:10.1007/s12517-018-4123-0

Gao, F. Q. (2019). Use of Numerical Modeling for Analyzing Rock Mechanic Problems in Underground Coal Mine Practices. *J. Min. Strata Control. Eng.* 1 (1), 013004. doi:10.13532/j.jmsce.cn10-1638/td.2019.02.009

Han, Z.-Z., Liu, H., Song, Z.-G., Zhong, W.-J., Han, C., Han, M., et al. (2018). Geochronology, Geochemistry, and Tectonic Implications of Upper Silurian - Lower Devonian Meta-Sedimentary Rocks from the Jiangyu Group in Eastern Jilin Province, Northeast China. *Can. J. Earth Sci.* 55, 490–504. doi:10.1139/cjes-2017-0260

He, S., Li, H., Qin, Q., and Long, S. (2021). Influence of Mineral Compositions on Shale Pore Development of Longmaxi Formation in the Dingshan Area, Southeastern Sichuan Basin, China. *Energy Fuels* 35 (13), 10551–10561. doi:10.1021/acs.energyfuels.1c01026

He, S., Qin, Q. R., Li, H., and Wang, S. L. (2022b). Deformation Differences in Complex Structural Areas in the Southern Sichuan Basin and its Influence on Shale Gas Preservation: A Case Study of Changning and Luzhou Area. *Front. Earth Sci.* 9, 818155. doi:10.3389/feart.2021.818534

He, S., Qin, Q. R., Li, H., and Zhao, S. X. (2022a). Geological Characteristics of Deep Shale Gas in the Silurian Longmaxi Formation in the Southern Sichuan Basin, China. *Front. Earth Sci.* 9, 818543. doi:10.3389/feart.2021.818155

Hooker, J. N., Abu-Mahfouz, I. S., Meng, Q., and Cartwright, J. (2018). Fractures in Mudrocks: Advances in Constraining Timing and Understanding Mechanisms. *J. Struct. Geol.* 125, 166–173. doi:10.1016/j.jsg.2018.04.020

Hou, E. K., Cong, T., Xie, X. S., and Wei, J. B. (2020). Ground Surface Fracture Development Characteristics of Shallow Double Coal Seam Staggered Mining Based on Particle Flow. *J. Min. Strata Control. Eng.* 2 (1), 013521. doi:10.13532/j.jmsce.cn10-1638/td.2020.01.002

Hu, L. (2022a). A Review of Mechanical Mechanism and Prediction of Natural Fracture in Shale. *Arab. J. Geosci.* 15 (6), 474. doi:10.1007/s12517-022-09786-w

Ibrahim, M. I. M., Hariri, M. M., Abdullatif, O. M., Makkawi, M. H., and Elzain, H. (2017). Fractures System within Qusaiba Shale Outcrop and its Relationship to the Lithological Properties, Qasim Area, Central Saudi Arabia. *J. Afr. Earth Sci.* 133, 104–122. doi:10.1016/j.jafrearsci.2017.05.011

Jarvie, D. M., Hill, R. J., Ruble, T. E., and Pollastro, R. M. (2007). Unconventional Shale-Gas Systems: The Mississippian Barnett Shale of north-central Texas as One Model for Thermogenic Shale-Gas Assessment. *Bulletin* 91 (4), 475–499. doi:10.1306/12190606068

Jiang, T., Zhang, J., and Wu, H. (2017). Effects of Fractures on the Well Production in a Coalbed Methane Reservoir. *Arab. J. Geosci.* 10 (22), 494. doi:10.1007/s12517-017-3283-7

Jin, Z., Nie, H., Liu, Q., Zhao, J., and Jiang, T. (2018). Source and Seal Coupling Mechanism for Shale Gas Enrichment in Upper Ordovician Wufeng Formation - Lower Silurian Longmaxi Formation in Sichuan Basin and its Periphery. *Mar. Pet. Geology.* 97, 78–93. doi:10.1016/j.marpetgeo.2018.06.009

Kang, H. P. (2021). Temporal Scale Analysis on Coal Mining and Strata Control Technologies. *J. Min. Strata Control. Eng.* 3 (1), 013538. doi:10.13532/j.jmsce.cn10-1638/td.20200814.001

Laubach, S. E., Olson, J. E., and Gross, M. R. (2009). Mechanical and Fracture Stratigraphy. *Bulletin* 93, 1413–1426. doi:10.1306/07270909094

Li, H. (2022b). Research Progress on Evaluation Methods and Factors Influencing Shale Brittleness: A Review. *Energ. Rep. Online* 8, 4344–4358. doi:10.1016/j.egyr.2022.03.120

Li, H., Qin, Q., Zhang, B., Ge, X., Hu, X., Fan, C., et al. (2020). Tectonic Fracture Formation and Distribution in Ultradeep marine Carbonate Gas Reservoirs: a Case Study of the Maokou Formation in the Jiulongshan Gas Field, Sichuan basin, Southwest China. *Energy Fuels* 34, 14132–14146. doi:10.1021/acs.energyfuels.0c03327

Li, H. (2021). Quantitative Prediction of Complex Tectonic Fractures in the Tight sandstone Reservoirs: a Fractal Method. *Arab. J. Geosci.* 14, 1986. doi:10.1007/s12517-021-08344-0

Li, H., Tang, H. M., and Zheng, M. J. (2019a). Micropore Structural Heterogeneity of Siliceous Shale Reservoir of the Longmaxi Formation in the Southern Sichuan Basin, China. *Minerals* 9, 548. doi:10.3390/min9090548

Li, H., Tang, H., Qin, Q., Zhou, J., Qin, Z., Fan, C., et al. (2019b). Characteristics, Formation Periods and Genetic Mechanisms of Tectonic Fractures in the Tight Gas Sandstones Reservoir: A Case Study of Xujiahe Formation in YB Area, Sichuan Basin, China. *J. Pet. Sci. Eng.* 178, 723–735. doi:10.1016/j.petrol.2019.04.007

Li, J., Qin, Q., Li, H., Wan, Y., and Wan, Y. F. (2022b). Numerical Simulation of the Stress Field and Fault Sealing of Complex Fault Combinations in Changning Area, Southern Sichuan Basin, China. *Energ. Sci. Eng.* 10 (2), 278–291. doi:10.1002/ese3.1044

Li, J., Qin, Q., Li, H., and Zhao, S. (2022a). Paleotectonic Stress Field Modeling and Fracture Prediction of the Longmaxi Formation in the N216 Well Block, Southern Sichuan Basin, China. *Arab. J. Geosci.* 15, 347. doi:10.1007/s12517-022-09616-z

Li, S., Santosh, M., Zhao, G., Zhang, G., and Jin, C. (2012). Intracontinental Deformation in a Frontier of Super-convergence: a Perspective on the Tectonic Milieu of the South China Block. *J. Asian Earth Sci.* 49, 313–329. doi:10.1016/j.jseaes.2011.07.026

Ma, X., Wang, H., Zhou, S., Shi, Z., and Zhang, L. (2021). Deep Shale Gas in China: Geological Characteristics and Development Strategies. *Energ. Rep.* 7, 1903–1914. doi:10.1016/j.egyr.2021.03.043

Melchin, M. J., and Holmden, C. (2006). Carbon Isotope Chemostratigraphy in Arctic Canada: Sea-Level Forcing of Carbonate Platform Weathering and Implications for Hirnantian Global Correlation. *Palaeogeogr. Palaeoclimatol. Palaeoecol.* 234 (2), 186–200. doi:10.1016/j.palaeo.2005.10.009

Mourgues, R., Bureau, D., Bodet, L., Gay, A., and Gressier, J. B. (2012). Formation of Conical Fractures in Sedimentary Basins: Experiments Involving Pore Fluids and Implications for sandstone Intrusion Mechanisms. *Earth Planet. Sci. Lett.* 313, 67–78. doi:10.1016/j.epsl.2011.10.029

Nie, H., He, Z., Wang, R., Zhang, G., Chen, Q., Li, D., et al. (2020). Temperature and Origin of Fluid Inclusions in Shale Veins of Wufeng-Longmaxi Formations, Sichuan Basin, south China: Implications for Shale Gas Preservation and Enrichmentfluid Inclusions in Shale Veins of Wufeng-Longmaxi Formations, Sichuan Basin, south China: Implications for Shale Gas Preservation and Enrichment. *J. Pet. Sci. Eng.* 193, 107329. doi:10.1016/j.petrol.2020.107329

Nie, H. K., and Jin, Z. J. (2016). Source Rock and Cap Rock Controls on the Upper Ordovician Wufeng Formation-Lower Silurian Longmaxi Formation Shale Gas Accumulation in the Sichuan Basin and its Peripheral Areas. *Acta Geol. Sin.* 90, 1059–1060. doi:10.1111/1755-6724.12752

Nie, H. K., Sun, C. X., Liu, G. X., Du, W., and He, Z. L. (2018). Dissolution Pore Types of the Wufeng Formation and the Longmaxi Formation in the Sichuan Basin, South China: Implications for Shale Gas Enrichment. *Mar. Petrol. Geol.* 101, 243–251. doi:10.1016/j.marpetgeo.2018.11.042

Qie, L., Shi, Y. N., and Liu, J. G. (2021). Experimental Study on Grouting Diffusion of Gangue Solid Filling Bulk Materials. *J. Min. Strata Control. Eng.* 3 (2), 023011. doi:10.13532/j.jmsce.cn10-1638/td.20201111.001

ReinersP.W.SpellT.L.NicolescuS.and ZanettiK. A (2004). Zircon (U-Th)/He Thermochronometry: He Diffusion and Comparisons with 40Ar/39Ar Dating. *Geochim. Cosmochim* 68, 1857–1887. doi:10.1016/j.gca.2003.10.021

Schwartzkopff, A. K., Melkoumian, N. S., and Xu, C. (2017). Fracture Mechanics Approximation to Predict the Breakdown Pressure Using the Theory of Critical Distances. *Int. J. Rock Mech. Mining Sci.* 95, 48–61. doi:10.1016/j.ijrmms.2017.03.006

Shan, S. C., Wu, Y. Z., Fu, Y. K., and Zhou, P. H. (2021). Shear Mechanical Properties of Anchored Rock Mass under Impact Load. *J. Min. Strata Control. Eng.* 3 (4), 043034. doi:10.13532/j.jmsce.cn10-1638/td.20211014.001

Shi, X., Wang, J., Liu, G., Yang, L., Ge, X., and Jiang, S. (2016). Application of Extreme Learning Machine and Neural Networks in Total Organic Carbon Content Prediction in Organic Shale with Wire Line Logs. *J. Nat. Gas Sci. Eng.* 33, 687–702. doi:10.1016/j.jngse.2016.05.060

Smeraglia, L., Mercuri, M., Tavani, S., Pignalosa, A., Kettermann, M., Billi, A., et al. (2021). 3D Discrete Fracture Network (DFN) Models of Damage Zone Fluid Corridors within a Reservoir-Scale normal Fault in Carbonates: Multiscale Approach Using Field Data and UAV Imagery. *Mar. Pet. Geology.* 126, 104902. doi:10.1016/j.marpetgeo.2021.104902

Song, J. F., Lu, C. P., Li, Z. W., Ou, Y. G. C., Cao, X. M., and Zhou, F. L. (2021). Characteristics of Stress Distribution and Microseismic Activity in Rock Parting Occurrence Area. *J. Min. Strata Control. Eng.* 3 (4), 043518. doi:10.13532/j.jmsce.cn10-1638/td.20210607.002

Wang, J., and Wang, X. L. (2021). Seepage Characteristic and Fracture Development of Protected Seam Caused by Mining Protecting Strata. *J. Min. Strata Control. Eng.* 3 (3), 033511. doi:10.13532/j.jmsce.cn10-1638/td.20201215.001

Wang, R., Hu, Z., Long, S., Liu, G., Zhao, J., Dong, L., et al. (2019). Differential Characteristics of the Upper Ordovician-Lower Silurian Wufeng-Longmaxi Shale Reservoir and its Implications for Exploration and Development of Shale Gas In/around the Sichuan Basin. *Acta Geologica Sinica - English Edition* 93 (3), 520–535. doi:10.1111/1755-6724.13875

Wang, R., Hu, Z., Sun, C., Liu, Z., Zhang, C., Gao, B., et al. (2018). Comparative Analysis of Shale Reservoir Characteristics in the Wufeng-Longmaxi (O3w-S1l) and Niutitang (Є1n) Formations: A Case Study of wells JY1 and TX1 in the southeastern Sichuan Basin and its Neighboring Areas, Southwestern China. *Interpretation* 6 (4), SN31–SN45. doi:10.1190/int-2018-0024.1

Wang, R. Y., Nie, H. K., Hu, Z. Q., Liu, G. X., Xi, B. B., and Liu, W. X. (2020). Controlling Effect of Pressure Evolution on Shale Gas Reservoirs: A Case Study of the Wufeng-Longmaxi Formation in the Sichuan Basin. *Nat. Gas Ind.* 40 (10), 1–11. doi:10.3787/j.issn.1000-0976.2020.10.001

Wang, S., Li, H., Lin, L., and Yin, S. (2022). Development Characteristics and Finite Element Simulation of Fractures in Tight Oil sandstone Reservoirs of Yanchang Formation in Western Ordos Basin. *Front. Earth Sci.* 9, 823855. doi:10.3389/feart.2021.823855

Xie, J., Qin, Q., and Fan, C. (2019). Quantitative Prediction of Fracture Distribution of the Longmaxi Formation in the Dingshan Area, China Using FEM Numerical Simulation. *Acta Geologica Sinica - English Edition* 93 (6), 1662–1672. doi:10.1111/1755-6724.13815

Xu, S., Gou, Q., Hao, F., Zhang, B., Shu, Z., Lu, Y., et al. (2020). Shale Pore Structure Characteristics of the High and Low Productivity wells, Jiaoshiba Shale Gas Field, Sichuan Basin, China: Dominated by Lithofacies or Preservation Condition? *Mar. Pet. Geology.* 114, 104211. doi:10.1016/j.marpetgeo.2019.104211

Yan, D., Chen, D., Wang, Q., Wang, J., and Wang, Z. (2009). Carbon and Sulfur Isotopic Anomalies across the Ordovician-Silurian Boundary on the Yangtze Platform, South China. *Palaeogeogr. Palaeoclimatol. Palaeoecol.* 274 (1-2), 32–39. doi:10.1016/j.palaeo.2008.12.016

Yang, R., He, S., Hu, Q. H., Sun, M. D., Hu, D. F., and Yi, J. Z. (2017). Applying SANS Technique to Characterize Nano-Scale Pore Structure of Longmaxi Shale, Sichuan Basin (China). *Fuel* 197, 91–99. doi:10.1016/j.fuel.2017.02.005

Yin, S., Lv, D., Jin, L., and Ding, W. (2018). Experimental Analysis and Application of the Effect of Stress on continental Shale Reservoir Brittleness. *J. Geophys. Eng.* 15 (2), 478–494. doi:10.1088/1742-2140/aaa5d2

Yin, S., and Wu, Z. (2020). Geomechanical Simulation of Low-Order Fracture of Tight sandstone. *Mar. Pet. Geology.* 117, 104359. doi:10.1016/j.marpetgeo.2020.104359

Yu, X., Bian, J. Q., and Liu, C. Y. (2022). Determination of Energy Release Parameters of Hydraulic Fracturing Roof Near Goaf Based on Surrounding Rock Control of Dynamic Pressure Roadway. *J. Min. Strata Control. Eng.* 4 (1), 013016. doi:10.13532/j.jmsce.cn10-1638/td.20210908.001

Yu, X. Y., Wang, Z. S., Yang, Y., and Mao, X. W. (2021). Numerical Study on the Movement Rule of Overburden in Fully Mechanized Caving Mining with Thick Depth and High Mining Height. *J. Min. Strata Control. Eng.* 3 (1), 013533. doi:10.13532/j.jmsce.cn10-1638/td.20200715.001

Zhang, K., Jia, C., Song, Y., Jiang, S., Jiang, Z., Wen, M., et al. (2020a). Analysis of Lower Cambrian Shale Gas Composition, Source and Accumulation Pattern in Different Tectonic Backgrounds: A Case Study of Weiyuan Block in the Upper Yangtze Region and Xiuwu Basin in the Lower Yangtze Region. *Fuel* 263, 115978. doi:10.1016/j.fuel.2019.115978

Zhang, K., Jiang, S., Zhao, R., Wang, P., Jia, C., and Song, Y. (2022). Connectivity of Organic Matter Pores in the Lower Silurian Longmaxi Formation Shale, Sichuan Basin, Southern China: Analyses from Helium Ion Microscope and Focused Ion Beam Scanning Electron Microscope. *Geol. J.* 1-13, 4387. doi:10.1002/gj.4387

Zhang, K., Peng, J., Liu, W. W., Li, B., Xia, Q. S., Cheng, S. H., et al. (2020b). The Role of Deep Geofluids in the Enrichment of Sedimentary Organic Matter: a Case Study of the Late Ordovician-Early Silurian in the Upper Yangtze Region and Early Cambrian in the Lower Yangtze Region, south China. *Geofluids* 2020, 8868638. doi:10.1155/2020/8868638

Zhang, X. J., He, J. H., Deng, H. C., Fu, M. Y., Xiang, Z. H., Peng, X. F., et al. (2021). Controls of Interlayers on the Development and Distribution of Natural Fractures in Lacustrine Shale Reservoirs: A Case Study of the Da'anzhai Member in the Fuling Area in the Eastern Sichuan Basin. *J. Petrol. Sci. Eng.* 208, 109224. doi:10.1016/j.petrol.2021.109224

Zhu, Q. Y., Dai, J., Yun, F. F., Zhai, H. H., Zhang, M., and Feng, L. R. (2022). Dynamic Response and Fracture Characteristics of Granite under Microwave Irradiation. *J. Min. Strata Control. Eng.* 4 (1), 019921. doi:10.13532/j.jmsce.cn10-1638/td.20210926.001

Conflict of Interest: Author SZ was employed by the company PetroChina Southwest Oil & Gas Field Company.

The remaining authors declare that the research was conducted in the absence of any commercial or financial relationships that could be construed as a potential conflict of interest.

The reviewer HD declared a shared affiliation with the author JH to the handling editor at the time of review.

Publisher's Note: All claims expressed in this article are solely those of the authors and do not necessarily represent those of their affiliated organizations, or those of the publisher, the editors and the reviewers. Any product that may be evaluated in this article, or claim that may be made by its manufacturer, is not guaranteed or endorsed by the publisher.